VOLUME 119, NUMBER 39
OCTOBER 1, 1997

JOURNAL OF THE AMERICAN CHEMICAL SOCIETY

ω-Amino Acids in Peptide Design. Crystal Structures and Solution Conformations of Peptide Helices Containing a β-Alanyl-γ-Aminobutyryl Segment

I. L. Karle,*,† Animesh Pramanik,‡ Arindam Banerjee,‡ Surajit Bhattacharjya,‡ and P. Balaram*,‡

Contribution from the Laboratory for the Structure of Matter, Naval Research Laboratory, Washington, DC 20375-5341, and Molecular Biophysics Unit, Indian Institute of Science, Bangalore 560 012, India

Received February 21, 1997[⊗]

Abstract: Insertion of achiral ω-amino acids into peptide sequences results in replacement of scissile peptide bonds by proteolytically stable C−C bonds. This provides a convenient means of creating peptidomimetics. The present study establishes the preservation of helical structures in octa- and undecapeptides with centrally located β- and γ-amino acids in the sequence. X-ray diffraction analyses of single crystals and NMR studies have been used to investigate the extent of perturbations of a regular 3_{10}- or α-helix by the introduction of $(-CH_2-)_n$ groups into the backbone by the use of the β-Ala-γ-Abu segment (β-Ala = β-alanine, γ-Abu = γ-aminobutyric acid), which is formally homomorphous with a $(Gly)_3$ segment. In crystals, the octapeptide Boc-Leu-Aib-Val-β-Ala-γ-Abu-Leu-Aib-Val-OMe (**1**) and the undecapeptide Boc-Leu-Aib-Val-β-Ala-γ-Abu-Leu-Aib-Val-Ala-Leu-Aib-OMe (**2**) retain their helical motifs with minor bulges. Five new types of $4 \rightarrow 1$, $5 \rightarrow 1$, and $6 \rightarrow 1$ hydrogen bond rings are formed with up to three extra CH_2 moieties. Cell parameters for peptide **1** are space group $P2_12_12_1$ with $a = 11.506$ (1) Å, $b = 16.600$ (1) Å, $c = 27.362(1)$ Å, and $R = 6.1\%$ for 2696 data measured $>4\sigma(F)$; for the undecapeptide **2**, the space group is $P2_1$ with $a = 8.605$ (3) Å, $b = 22.806$ (4) Å, $c = 19.014$ (3) Å, $\beta = 101.47(2)°$, and $R = 7.5\%$ for 3797 data measured $>4\sigma(F)$. Helical conformations in solution are also maintained for peptide **2** as is evident from NMR studies in $CDCl_3$, which suggest that the centrally positioned, flexible β-Ala-γ-Abu segment can be comfortably accommodated into helical structures adopting *gauche* conformations about specific C−C bonds of the poly(methylene) units. Twenty structures for backbone conformations generated from MD simulations using NMR-derived contraints, superpose with a low RMSD value (0.78 ± 0.05 Å), further indicating that in these peptides the conformational flexibility of the β-Ala-γ-Abu segment is limited and confined to largely helical conformations.

Incorporation of ω-amino acids into polypeptides provides a convenient means of inserting additional methylene groups into peptide chains.[1] Amide bond replacements are also useful in generating peptide analogues which are resistant to proteolytic cleavage.[2] The replacement of peptide bonds by ethylene units results in interruption of regular patterns of intramolecular hydrogen bonds. Systematic investigations of the effects of incorporation of ω-amino acids on the stereochemistry of polypeptide chains are therefore essential as a prelude to rational design of peptides with an expanded repertoire of amino acid building blocks. The ability of poly(methylene) chains to adopt *gauche* ($\theta = 60°$) and *trans* ($\theta = 180°$) conformations about the C−C bonds[3] suggests that oligomethylene units can indeed be inserted into the folded peptide chain.[1a] For example, the

* To whom correspondence should be addressed.
† Naval Research Laboratory.
‡ Indian Institute of Science.
⊗ Abstract published in *Advance ACS Abstracts,* September 15, 1997.

S0002-7863(97)00566-0 CCC: $14.00

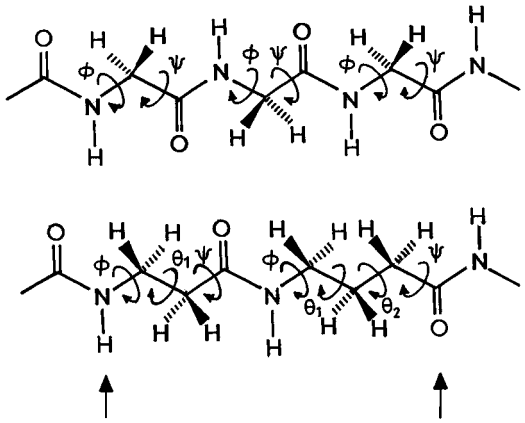

Figure 1. Comparison of homomorphic segment (a) Gly-Gly-Gly with (b) β-Ala-γ-Abu. The nomenclature of dihedral angles defined by backbone atoms is indicated in both cases.

backbone dihedral angles for an L-amino acid residue in a right-handed α-helical conformation are $\phi = -57°$, $\psi = -47°$, and $\omega = 180°$.[4] In principle, such a pattern of backbone dihedral angles is compatible with insertion of contiguous methylene groups. Figure 1 illustrates the replacement of a three residue, $(Gly)_3$, segment in a polypeptide chain with a β-alanyl-γ-aminobutyryl (β-Ala-γ-Abu) unit. In both cases, the number of atoms contributing to the segment is nine. However, the two central peptide units in the tri-α-amino acid segment are now substituted by one central peptide bond in the β-Ala-γ-Abu segment, with an accompanying change in the "register" of the amide bond. As a part of a systematic investigation of the effects of ω-amino acid incorporation into helical peptide sequences, we have examined eight- and 11-residue peptides containing internal β-Ala-γ-Abu segments. This paper presents the crystal structures of Boc-Leu-Aib-Val-β-Ala-γ-Abu-Leu-Aib-Val-OMe (**1**) and Boc-Leu-Aib-Val-β-Ala-γ-Abu-Leu-Aib-Val-Ala-Leu-Aib-OMe (**2**), which establish preservation of a helical backbone despite the insertion of β- and γ-amino acids. NMR studies in $CDCl_3$ confirm the retention of a helical conformation in solution. Sequence **2** was designed after inspection of the crystal structure of peptide **1**, which revealed a helix terminating motif formed by reversal of helix sense at the penultimate Aib residue. The third Aib residue was therefore positioned at the C-terminal in **2**.

Experimental Section

Peptide Synthesis. Peptides were synthesized by conventional solution phase methods by using a fragment condensation strategy. The Boc group was used for N-terminal protection, and the C-terminus was protected as a methyl ester. Deprotections were performed using 98% formic acid or saponification, respectively. Couplings were mediated by dicyclohexylcarbodiimide−1-hydroxybenzotriazole (DCC/HOBT). All the intermediates were characterized by ^{1}H NMR (80 and 400 MHz) and thin layer chromatography (TLC) on silica gel. The final peptide was purified by medium-pressure liquid chromatography (MPLC) and high-performance liquid chromatography (HPLC) on reverse phase C-18 columns and fully characterized by 400 MHz ^{1}H-NMR.

Boc-γ-Abu-Leu-Aib-Val-OMe (3): To 5.67 g (13.3 m mol) of Boc-Leu-Aib-Val-OMe[5] was added 15 mL of 98% formic acid, and the removal of the Boc group was monitored by TLC. After 8 h, the formic acid was removed *in vacuo*. The residue was taken in water (20 mL) and washed with diethyl ether (2 × 20 mL). The pH of the aqueous solution was then adjusted to 8 with sodium bicarbonate and extracted with ethyl acetate (3 × 30 mL). The extracts were pooled, washed with saturated brine, dried over sodium sulfate, and concentrated to 5 mL of a highly viscous gum that gives a ninhydrin positive test. The tripeptide free base was added to an ice-cooled solution of Boc-γ-Abu-OH (2.09 g, 10.3 mmol) in 10 mL of DMF, followed by 2.1 g (10.5 mmol) of DCC and 1.39 g (10.3 mmol) of HOBT. The reaction mixture was stirred for 3 days. The residue was taken in ethyl acetate (60 mL), and *N*,*N*′-dicyclohexylurea (DCU) was filtered off. The organic layer was washed with 2 N HCl (3 × 50 mL), 1 M sodium carbonate (3 × 50 mL), and brine 2 × 50 mL), dried over sodium sulfate, and evaporated *in vacuo* to yield 4.1 g (78%) of a white solid: mp 140 °C; 80 MHz ^{1}H NMR ($CDCl_3$, δ ppm) 0.81−0.98 (12H, m, Leu C$^\delta$H$_3$ and Val C$^\gamma$H$_3$), 1.37 (9H, s, Boc CH$_3$), 1.44 (3H, s, Aib C$^\beta$H$_3$), 1.51 (3H, s, Aib C$^\beta$H$_3$), 1.69−1.71 (3H, m, Leu C$^\gamma$H and Leu C$^\beta$H), 1.82−2.00 (2H, m, γ-Abu C$^\beta$H), 2.15−2.25 (3H, m, Val C$^\beta$H and γ-Abu C$^\alpha$H), 3.10 (2H, m, γ-Abu C$^\gamma$H), 3.66 (3H, s, OCH$_3$), 4.25−4.45 (2H, m, Leu C$^\alpha$H and Val C$^\alpha$H), 4.89 (1H, m, γ-Abu NH), 6.66 (1H, d, Leu NH/ValNH), 6.94 (1H, s, Aib NH), 7.05 (1H, d, ValNH/Leu NH).

Boc-Leu-Aib-Val-β-Ala-OMe (4): Boc-Leu-Aib-Val-OH[5] (1.12 g, 2.7 mmol) in 15 mL of DMF was cooled in an ice bath, and H-β-Ala-OMe (isolated from 0.77 g (5.5 mmol) of the hydrochloride by neutralization, subsequent extraction with ethyl acetate, and concentration (5 mL)) was added, followed immediately by 0.54 g (2.7 mmol) of DCC and 0.41 g (2.7 mmol) of HOBT. The reaction mixture was stirred for 3 days. The residue was taken in ethyl acetate (50 mL), and the DCU was filtered off. The organic layer was washed with 2 N HCl (3 × 50 mL), 1 M sodium carbonate (3 × 50 mL), and brine (2 × 50 mL), dried over anhydrous sodium sulfate, and evaporated *in vacuo* to yield 1.00 g (63%) of a gummy material: ^{1}H NMR (80 MHz, $CDCl_3$, δ ppm) 0.78−0.86 (12H, m, Leu C$^\delta$H3 and Val C$^\gamma$H$_3$), 1.31 (12H, s, Boc CH$_3$), 1.41 (6H, s, Aib C$^\beta$H), 1.75−1.82 (3H, m, Leu C$^\gamma$H and Leu C$^\beta$H), 1.98 (1H, m, Val C$^\beta$H), 2.15 (2H, m, β-Ala C$^\alpha$H), 313 (2H, m, β-Ala C$^\beta$H), 3.52 (3H, s, OCH$_3$), 3.76 (1H, m, Leu C$^\alpha$H/Val C$^\alpha$H), 4.16 (1H, m, Leu C$^\alpha$H/ValC$^\alpha$H), 5.40 (1H, d, Leu NH), 6.68 (1H, d, Val NH), 6.84 (1H, s, Aib NH), 7.16 (1H, m, β-Ala NH).

Boc-Leu-Aib-Val-β-Ala-γ-Abu-Leu-Aib-Val-OMe (1): 3 (1.29 g, 2.5 mmol) was deprotected with 98% formic acid and worked up as

(1) (a) Banerjee, A.; Pramanik, A.; Bhattacharjya, S.; Balaram, P. *Biopolymers* **1996**, *39*, 769−777. (b) Groeger, C.; Wenzel, H. L.; Tschesche, H. *Angew. Chem., Int. Ed. Engl.* **1993**, *32*, 898−900. (c) Dado, G. P.; Gellman, S. H. *J. Am. Chem. Soc.* **1994**, *116*, 1054−1062. (d) Pavone, V.; Di Blasio, B.; Lombardi, A.; Isernia, C.; Pedone, C.; Benedetti, E.; Valle, G.; Crisma, M.; Toniolo, C.; Kishore, R. *J. Chem. Soc., Perkin Trans 2* **1992**, 1233−1237. (e) Lombardi, A.; Saviano, M.; Nastri, F.; Maglio, O.; Mazzeo, M.; Pedone, C.; Iserina, C.; Pavone, V. *Biopolymers* **1996**, *38*, 683−691. (f) Lombardi, A.; Saviano, M.; Nastri, F.; Maglio, O.; Mazzeo, M.; Iserina, C.; Paolillo, L.; Pavone, V. *Biopolymers* **1996**, *38*, 693−703. (g) Karle, I. L.; Flippen-Anderson, J. L.; Sukumar, M.; Uma, K.; Balaram, P. *J. Am. Chem. Soc.* **1991**, *113*, 3952−3956.

(2) (a) Goodman, M; Ro, S. In *Burger's Medicinal Chemistry and Drug Discovery*; **1995**, Vol. 1 (Wolff, M. E., Ed.; John Wiley & Sons, Inc.: New York, 1995; Vol. 1, p 803. (b) Hruby, V. J. *Biopolymers* **1993**, *33*, 1079−1082. (c) Toniolo, C. *Int. J. Peptide Protein Res.* **1990**, *35*, 287−300. (d) Marraud, M.; Dupont, V.; Grand, V.; Zerkout, S.; Lecoq, A.; Boussard, G.; Vidal, J.; Collet, A.; Aubry, A. *Biopolymers* **1993**, *33*, 1135−1148. (e) Guichard, G.; Benkirane, N.; Graff, R.; Muller, S.; Briand, J. P. *Peptide Res.* **1994**, *7*, 308−321.

(3) (a) Navarro, E.; Tereshka, V.; Subirana, J. A.; Puiggalía, J. *Biopolymers* **1995**, *36*, 711−722. (b) Alemán, C.; Navarro, E.; Puiggalía, J. *J. Org. Chem.* **1995**, *60*, 6135−6140. (c) Navarro, E.; Alemán, C.; Puiggalía, J. *J. Am. Chem. Soc.* **1995**, *117*, 7307−7310.

(4) (a) Abbreviations used: Aib, α-aminoisobutyric acid; β-Ala, β-alanine, γ-Abu, γ-aminobutyric acid. (b) Standard dihedral angle nomenclature follows the IUPAC-IUB Commission on Biochemical Nomenclature: *Biochemistry* **1970**, *9*, 3471−3479. (c) Nomenclature for the backbone dihedral angles in β-Ala and γ-Abu is as described in Figure 1. The C$^\alpha$−CO bond is designated as ψ, while N−C$^\omega$ bond is designated as ϕ in the ω-amino acids. The C−C dihedral angles are defined as θ_n with numbering beginning from the N-terminus. It may be noted that the methylene carbon adjacent to the carboxyl group is labeled as C$^\alpha$ in the ω-amino acids. This results in C$^\gamma$H$_2$ preceding C$^\beta$H$_2$ when the peptide chain is conventionally read from N-terminus to C-terminus. (c) We use the term *peptide bond* also to describe amide linkages involving ω-amino acids. It may be noted that Emil Fischer's introduction[4d] of the term polypeptide was not restricted to linkages involving α-amino acids only. (d) "Den namen polypeptide habe ich vorgeschlagen fur die Produkte, die durch amidartige Verkettung von Aminosauren entstehen...": Fischer, E. *Ber. Dtsch. Chem. Ges.* **1906**, *39*, 530. See also: *Chemistry of the amino acids*; Greenstein, J. P., Winitz, M., Eds.; Krieger: Malaber, FL, 1984; Vol. 2, pp 763, 1816a.

(5) Karle, I. L.; Banerjee, A.; Bhattacharjya, S.; Balaram, P. *Biopolymers* **1996**, *38*, 515−525.

Table 1. Crystal and Diffraction Parameters[a]

peptide	**1** (octa)	**2** (undeca)
empirical formula	$C_{43}H_{78}N_8O_{11}$	$C_{56}H_{101}N_{11}O_{14}\cdot C_4H_8O_2$
crystallizing solvent	EtOAc/*n*-hexane/MeOH	EtOAc/*n*-heptane
cocrystallized solvent		ethyl acetate
color/habit	colorless thin plates	colorless needles
crystal size (mm)	0.50 × 0.13 × 0.14	0.90 × 0.18 × 0.12
space group	$P2_12_12_1$	$P2_1$
a (Å)	11.506(1)	8.605(3)
b (Å)	16.600(1)	22.806(4)
c (Å)	27.362(2)	19.014(3)
β (deg)	90.0	101.47(2)
V (Å^3)	5226.1	3657.1(15)
Z	4	2
mol wt	883.1	1232.5
density, calcd (g/cm^3)	1.122	1.119
F(000)	1920	1252
T (°C)	+21	−50[b]
no. of unique reflns	4645	5571
no. of obsd reflns $\lvert F_o\rvert > 4\sigma(F)$	2696	3797
weights	0.00025	unit
final *R* (obsd data) (%)	6.1	7.5
S	1.38	2.01
resolution (Å)	0.9	0.9
data/param ratio	4.8:1.0	5.0:1.0
no. of params	559	753

[a] For both crystals, Cu Kα radiation (λ = 1.541 78 Å) was used with a $\theta/2\theta$ scan, a scan width of 2.0° + 2θ($\alpha_1 - \alpha_2$) and a scan speed of 10 deg/min. Standard reflections were read after every 97 measurements. Standards remained constant (within 3%). Both crystals were coated with microscope immersion oil. [b] Undecapeptide crystal not stable at room temperature.

reported in the preparation of **3**. This was coupled to 0.98 g (2.1 mmol) of Boc-Leu-Aib-Val-*β*-Ala-OH, obtained by the saponification of **4**. DMF (15 mL), 0.60 g of DCC, and 0.34 g of HOBT were used for this coupling. After 3 days the reaction was worked up as usual to yield 1.74 g of the crude peptide. The peptide was purified on a reverse phase C-18 MPLC column using methanol−water gradients (60%−95%): mp 92−93 °C; $[\alpha]^{26}_{589}$ −20.00° (*c* = 1 gm/100 mL, MeOH); 400 MHz ^{1}H NMR [$(CD_3)_2SO$, δ ppm] 0.79 (6H, m, Val C$^\gamma$H$_3$), 0.82 (6H, m, Val C$^\gamma$H$_3$), 0.86 (12H, m, Leu C$^\delta$H$_3$), 1.42 (9H, s, Boc CH$_3$), 1.49 (6H, m, Leu C$^\beta$H$_2$ and C$^\gamma$H), 1.56 (1H, m, *γ*-Abu C$^\beta$H), 1.63 (1H, m, *γ*-Abu C$^\beta$H), 1.94 (1H, m, Val C$^\gamma$H), 2.00 (1H, m, Val C$^\gamma$H), 2.12 (2H, m, *γ*-Abu C$^\alpha$H), 2.22 (1H, m, *β*-Ala C$^\alpha$H), 2.98 (2H, m, *γ*-Abu C$^\gamma$H), 3.18 (1H, m, *β*-Ala C$^\beta$H), 3.22 (1H, m, *β*-Ala C$^\beta$H), 3.93 (1H, m, Leu1 C$^\alpha$H), 4.01 (1H, m, Val C$^\alpha$H), 4.08 (1H, m, Val C$^\alpha$H), 4.17 (1H, m, Leu C$^\alpha$H), 6.87 (1H, d, Leu NH), 6.96 (1H, d, Val NH), 7.24 (1H, d, Val NH), 7.83 (2H, m, *β*-Ala NH and *γ*-Abu NH), 8.01 (1H, d, Leu NH), 8.03 (1H, s, Aib NH), 8.22 (1H, s, AibNH).

Boc-Leu-Aib-Val-*β*-Ala-*γ*-Abu-Leu-Aib-Val-Ala-Leu-Aib-OMe (2): Boc-Ala-Leu-Aib-OMe[6] (0.44 g, 1.10 mmol) was deprotected with 98% formic acid and worked up as reported in the preparation of **3**. This was coupled to 0.48 g (0.55 m mol) of Boc-Leu-Aib-Val-*β*-Ala-*γ*-Abu-Leu-Aib-Val-OH, obtained by saponification of **1**. DMF (15 mL), 0.11 g of DCC, and 0.10 g of HOBT were used for this coupling. After 3 days the reaction was worked up as usual to yield 0.58 g of the crude peptide. The peptide was purified on a reverse phase C-18 MPLC column using methanol−water gradiants (60%−95%). The peptide was further subjected to HPLC purification on a Lichrosob reverse phase C-18 HPLC column (4 × 250 mm, particle size 10 *μ*m, flow rate 1.5 mL/min) and eluted on a linear gradient of methanol−water (60%-95%) with a retention time of 22 min. The peptide was homogeneous on a reverse phase C-18 (5 *μ*m) column and fully characterized by NMR (see Results): mp 105−106 °C; $[\alpha]^{26}_{589} = -254.00°$ (*c* = 0.22 gm/100 mL, MeOH).

X-ray Diffraction. Crystals were grown from ethyl acetate/*n*-hexane solution by slow evaporation. Crystal and data collection parameters are listed in Table 1. Both the octapeptide and undecapeptide crystals were covered with microscope immersion oil upon removal from their mother liquor. The undecapeptide crystal needed to be cooled immediately to −50 °C by a cold stream of N_2 in order to remain stable during the X-ray data collection, while the octapeptide remained stable at room temperature.

The structure of the octapeptide was found quite routinely by direct phase determination, while the structure of the undecapeptide was solved with a vector search procedure[7] and partial structure expansion[8] contained in the PATSEE program which is an independent program compatible with SHELX 84 package of programs.[9] A successful model for the vector search for the undecapeptide was not found using fragments based on the known octapeptide structure. In retrospect, it was found that the conformations of the two peptides are quite diverse despite having the same sequence for residues 1−8. A model using 25 backbone and C$^\beta$ atoms in the C$^\alpha$4 to C$^\alpha$9 segment of Boc-Gly-Dpg-Pro-Val-Ala-Leu-Aib-Val-Ala-Leu-OMe[10] was entirely successful in the rotation, translation, and phase expansion procedure. Atoms for the entire peptide molecule were present in the first *E*-map. The cocrystallized ethyl acetate solvent was found in a subsequent difference map.

Full-matrix least-squares refinements with anisotropic thermal parameters were performed on the coordinates of C, N, and O atoms. Hydrogen atoms were placed in idealized positions and allowed to ride with the C or N atoms to which they are bonded. In the last cycles of refinement of the undecapeptide, some restraints were placed on the bond lengths of the ethyl acetate solvent molecule. The R factor of the octapeptide is 6.1% for 2696 data (greater than 4σ(*F*)); for the undecapeptide, the *R* factor is 7.5% for 3797 data (greater than 4σ(*F*)).

Fractional coordinates for the C, N, or O atoms for the octapeptide **1** and undecapeptide **2** are provided as Supporting Information.

NMR Experiments. All NMR studies were carried out on a Bruker AMX-400 spectrometer. Peptide concentrations were in the range 5−6 mM in $CDCl_3$. Resonance assignments were done using 2-D TOCSY, double-quantum filtered COSY, and ROESY spectra at 303 K. All the 2-D experiments were acquired using 1K data points, 512 increments, and 40−72 scans. The mixing time of ROESY and TOCSY experiments were set to 300 and 70 ms, respectively. The 2-D data were processed using Bruker's UXNMR software in a 1K × 1K data matrix. The FIDs were multiplied by a 90° phase-shifted square sinebell function prior to Fourier transformation.

(6) Uma, K. Modular design of synthetic protein mimics. Constuction of helices. Ph.D. Thesis, Indian Institute of Science, Bangalore, 1990.

(7) Egert, E.; Sheldrick, G. M. *Acta Crystallogr. A* **1985**, *41*, 262−268.

(8) Karle, J. *Acta Crystallogr. B* **1968**, *24*, 182−186.

(9) Sheldrick, G. M. SHELXTL PLUS, Release 4.2 for Siemens R3m/V Crystal Research System. Siemens Analytical X-ray Instruments, Madison, Wisconsin, WI, 1992.

(10) Karle, I. L.; Gurunath, R.; Prasad, S.; Kaul, R.; Balaji Rao, R.; Balaram, P. *J. Am. Chem. Soc.* **1995**, *117*, 9632−9637.

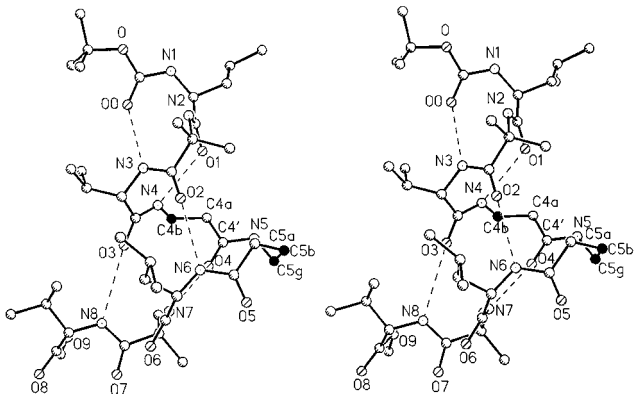

Figure 2. Stereodiagram of **1**. There is a helix reversal at the penultimate Aib7 residue and a 6 → 1 type hydrogen bond between N(8) and O(3). The darkened atoms in the backbone represent the C atoms of the extra CH_2 groups in β-Ala4 (C4b) and γ-Abu5 (C5b and C5g).

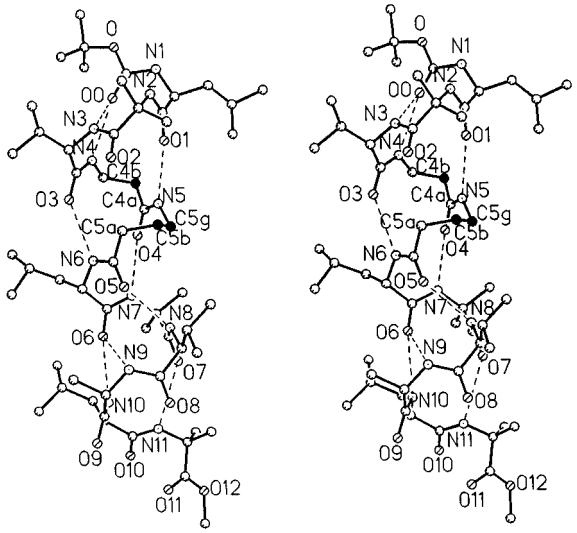

Figure 3. Stereodiagram of **2**, with three additional residues, Ala9-Leu10-Aib11, as compared to **1**. The helix is a mixed $3_{10}/\alpha$ type, without any helix reversal. The darkened atoms are the same as in **1** (C4b, C5b, and C5g).

Solvent perturbation experiments were performed to identify solvent exposed amide protons. A set of 1-D experiments were done in presence of increasing concentrations of dimethyl sulfoxide (0.5−10% v/v).

Constrained Molecular Dynamics. The NOE-derived distance constraints were used to obtain a 3-D structure of peptide **2**. All computations were performed on a Silicon Graphics Iris workstation using Biosym Software (INSIGHT II). MD simulations and energy minimizations were done using the DISCOVER module. The β-Ala and γ-Abu were constructed by modifying glycine residues. All other residues were available in the INSIGHT amino acid library. On the basis of the NOEs and H-bond information, a crude model of the peptide was built. The ϕ and ψ values of the model were initially fixed in a helical conformation ($\phi = -60°$, $\psi = -40°$, and $\omega = 180°$). However, the dihedral angles around the methylene bridges of β-Ala and γ-Abu (θ_1 and θ_2) were fixed in an extended conformation. The ends of the peptide were blocked by Boc and OMe groups. The consistent valence force field (CVFF)[11] was used with Morse harmonic potential energy terms for bond lengths and bond and dihedral angles, without any cross terms for charge−charge interactions. A dielectric constant of 1.0 was used, which may be a good approximation of a solvent like chloroform. A few cycles of unconstrained energy minimization using steepest descent were performed to relax short contacts in the initial structure.

(11) Dauber-Osguthorpe, P.; Roberts, V. A.; Osguthorpe, V. A.; Wolff, J.; Genest, M.; Hagler, A. T. *Proteins: Struct. Funct. Genet.* **1988**, *4*, 31−47.

Table 2. Torsional Angles (deg)[a,b] in Boc-LUV-β-Ala-γ-Abu-LUV-OMe (**1**)

residue	ϕ	ψ	ω	χ^1	χ^2	θ_1	θ_2
Leu1	−62	−28	−174	−73	+173		
					−65		
Aib2	−55	−33	−175				
Val3	−78	−17	−175	−69			
				−59			
β-Ala4[c]	−103	−162	−176			+76	
γ-Abu5[c]	−108	−146	−169			+58	+66
Leu6	−86	−18	−180	−72	+163		
					−70		
Aib7[d]	+49	+48	+178				
Val8	−53	−41	−174	−58			
				+179			

[a] The torsional angles for rotation about bonds of the peptide backbone (ϕ, ψ, and ω) and about bonds of the amino side chains (χ^n) are described in ref 4b. For the Boc group, values for torsional angles ψ' (C(1)−O−C(0)′−N(1)) and ω' (O−C(0)′−N(1)−C(1)$^\alpha$) are −176° and −175°, respectively. [b] Esd's ∼ 0.9°. [c] Torsions in the main chain about C$^\alpha$−C$^\beta$ and C$^\beta$−N(4) in β-Ala4 are represented by θ_1 and ϕ, and about C$^\alpha$−C$^\beta$, C$^\beta$−C$^\gamma$, and C$^\gamma$−N(5) in γ-Abu5 by θ_2, θ_1, and ϕ. [d] Helix reversal at Aib7.

Table 3. Torsional Angles (deg)[a,b] in Boc-LUV-β-Ala-γ-Abu-LUVALU-OMe (**2**)

residue	ϕ	ψ	ω	χ^1	χ^2	θ_1	θ_2
Leu1	−62	−35	−177	−153	+175		
					+17		
Aib2	−57	−38	−174				
Val3	−96	−43	+176	−48			
				−169			
β-Ala4[c]	−103	−107	−176			+78	
γ-Abu5[c]	−121	−121	−178			+63	+57
Leu6	−57	−37	−180	−72	+169		
					−69		
Aib7	−54	−36	−180				
Val8	−66	−45	−178	−61			
				+175			
Ala9	−68	−36	−173				
Leu10	−88	−11	180	−67	+172		
					−62		
Aib11	−57	+152	+177				

[a] The torsional angles for rotation about bonds of the peptide backbone (ϕ, ψ, and ω) and about bonds of the amino side chains (χ^n) are described in ref 4b. For the Boc group, values for torsional angles ψ' (C(1)−O−C(0)′−N1) and ω' (O−C(0)′−N(1)−C(1)$^\alpha$) are −170° and −175°, respectively. [b] Esd's ∼ 0.9°. [c] Torsions in the *main chain* about C$^\alpha$−C$^\beta$ and C$^\beta$−N(4) in β-Ala4 are represented by θ_1 and ϕ and about C$^\alpha$−C$^\beta$, C$^\beta$−C$^\gamma$, and C$^\gamma$−N(5) in γ-Abu5 by θ_2, θ_1, and ϕ as described in footnote 4c.

The geometry of the structure was checked to ensure that there were no distance or dihedral angle violations. This structure was further used for constrained MD simulations. All the backbone NOEs (intra- or inter-residue) were used as distance constraints in the MD simulation. Since the ROESY spectra yielded relatively poor NOE intensities, NOEs were scaled into only two distance categories; the relatively strong NOEs are fixed to a range of 2.0−3.0 Å; all other weak NOEs fall into a 2.8−3.5 Å distance range. No dihedral angles or hydrogen bonds were used in constrained simulations. A force constant of 20 kcal/mol was applied on all distance constraints as a penalty function for violation of distance criteria. The constrained MD simulations were performed for 100 ps at 300 K with a 10 ps equilibration time. Among the 50 structures generated, 20 of them superposed with low rmsd. These 20 structures were further examined for dihedral angles, hydrogen bonds, and restraint violations.

Results and Discussion

The Helices. The helical molecules **1** and **2** are shown in Figures 2 and 3, respectively. Torsional angles are listed in Tables 2 and 3, and hydrogen bond parameters are listed in

Table 4. Hydrogen Bonds in **1**

type	donor	acceptor	N···O, Å	H···O,[a] Å	C=O···N, deg
head-to-tail	N(1)	O(6)[b]	2.814	1.93	147
	N(2)	O(7)[b]	2.959	2.38	150
4 → 1	N(3)	O(0)	3.325	2.46	128
	N(4)	O(1)	2.959	2.12	127
interpeptide	N(5)	O(9)[c]	3.190	2.33	
5 → 1 (16-atom ring[d])	N(6)	O(2)	2.959	2.14	158
4 → 1 (12-atom ring[e])	N(7)	O(4)	2.835	2.03	165
6 → 1 (19-atom ring[f])	N(8)	O(3)	3.372	2.48	163

[a] Hydrogen atoms have been placed in idealized positions with N−H = 0.90 Å. [b] Symmetry equivalent $1.5 - x, -y, -0.5 + z$ to coordinates listed in Supporting Information. [c] Symmetry equivalent $1 - x, -0.5 + y, 1.5 - z$; possible hydrogen bond to methoxy O. [d] 5 → 1 plus backbone atoms C4B, C5B, and C5G from the β-Ala4 and γ-Abu5 residues. [e] 4 → 1 plus backbone atoms C5B and C5G from the γ-Abu5 residue. [f] 6 → 1 with helix reversal and backbone atoms C4B, C5B, and C5G from the β-Ala4 and γ-Abu5 residues.

Table 5. Hydrogen Bonds in **2**

type	donor	acceptor	N···O, Å	H···O,[a] Å	C=O···N, deg
head-to-tail	N(1)	O(9)[b]	2.822	2.16	152
	N(2)	O(10)[c]	2.910	2.21	147
4 → 1 transition	N(3)	O(0)	3.133	2.38	125
5 → 1	N(4)	O(0)	2.885	2.01	169
5 → 1 (14-atom ring[d])	N(5)	O(1)	2.826	1.93	161
4 → 1 (13-atom ring[e])	N(6)	O(3)	2.928	2.05	142
4 → 1 (12-atom ring[f])	N(7)	O(4)	2.761	1.88	148
4 → 1	N(8)	O(5)	2.992	2.24	129
4 → 1 transition	N(9)	O(6)	3.030	2.50	114
5 → 1	N(10)	O(6)	2.931	2.10	167
	N(11)	O(7)	3.178	2.53	143

[a] Hydrogen atoms have been placed in idealized positions with N−H = 0.90 Å. [b] Symmetry equivalent $x, y, -1 + z$. [c] Symmetry equivalent $-1 + x, y, -1 + z$. [d] 5 → 1 plus backbone atoms C4B, from the β-Ala4 residue. [e] 4 → 1 plus backbone atoms C4B, C5B, and C5G from the β-Ala4 and γ-Abu5 residue. [f] 4 → 1 plus backbone atoms C5B and C5G from the γ-Abu5 residues. [g] No hydrogen bonds are formed with the ethyl acetate cocrystallized solvent.

Tables 4 and 5. An immediately obvious difference in conformation, independent of the β-Ala-γ-Abu segment, is the helix reversal in **1** at the C^{α} atom of Aib7, which makes possible the 6 → 1 type hydrogen bond, N(8)H···O(3). Helix reversal of the 6 → 1 type have been found to occur at the penultimate Aib residues in peptide helices[12] and at the penultimate Gly or Asp residues in protein helices.[13] Hydrated (or solvated) 6 → 1 hydrogen bonds, in which a water molecule or an OH group from a solvent molecule forms a bridge between the C=O and NH groups in the peptide, have also been observed in crystals.[5] In the present octapeptide **1**, the 6 → 1 hydrogen bond has been modified in that the ring containing the N(8)H···O(3) hydrogen bond has three extra CH_2 groups in the backbone provided by the β-Ala-γ-Abu sequence, thus increasing the total number of atoms in the ring from 16 to 19 (Figure 4a). An addition of three residue to **1** produces **2**. The helix termination by formation of a Schellman motif in peptide helices

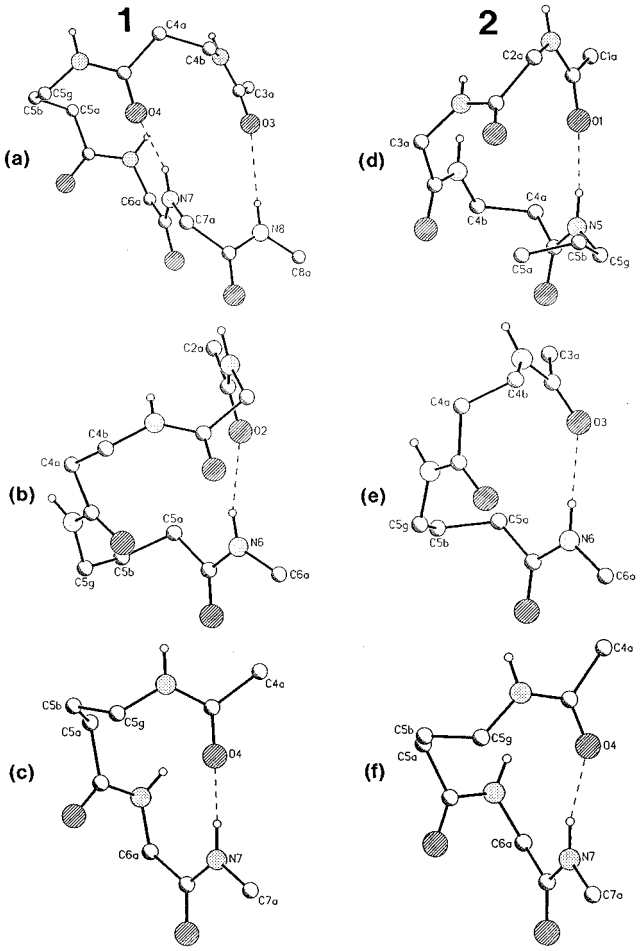

Figure 4. Unusual hydrogen bonds in helices of **1** (left) and **2** (right), with up to three additional CH_2 groups in the hydrogen bond ring structures, that derive from the β-Ala4-γ-Abu5 segment.

requires positive ϕ and ψ values at the penultimate residue, a feature facilitated by Aib at this position. In **1**, the terminating feature is formally analogous to the Schellman motif with additional insertion of methylene groups with the 6 → 1 hydrogen bonding. Since the Aib residue is removed from the penultimate position, no helix reversal occurs in **2**.

Aside from the helix reversal in **1** at Aib7, the remainder of the helix has three 4 → 1 type hydrogen bonds and one modified 5 → 1 type. It would have been an almost ideal 3_{10}-helix, consistent with octapeptides containing two Aib residues,[14] except for the insertion of the three extra CH_2 groups in β-Ala4-γ-Abu5 that result in a bulge in the helix, see atoms N(5), C(5G), and C(4G) in Figure 2. The N(5) atom is displaced sufficiently far from the helix axis, by the insertion of C(4B) so that it does not participate in any intramolecular H-bonds. It may form a hydrogen bond with O(9), part of the terminal OMe group of a neighboring molecule. The N(5)···O(9) distance of 3.19 Å and the N(5)H···O(9) distance of 2.33 Å are within the range of hydrogen bond distances observed for the helices containing one or more Aib residues.[14] The following N(6)H moiety forms an intramolecular hydrogen bond with O(2). The ring of 16 atoms can be described as a 5 → 1 type of hydrogen bond with the insertion of C(4B), C(5B), and C(5G) (Figure 4b). The next hydrogen bond, N(7)···O(4), is a 4 → 1 type with the insertion of C(5B) and C(5G) (Figure 4c). The torsional angles involving the inserted CH_2 groups are approximately +60°, see θ_n, in Table 2. It should be noted that the hydrogen bonds between

(12) (a) Karle, I. L.; Flippen-Anderson, J. L.; Uma, K.; Balaram, P. *Int. J. Pept. Protein Res.* **1993**, *42*, 401−410. (b) Banerjee, A.; Datta, S.; Pramanik, A.; Shamala, N.; Balaram, P. *J. Am. Chem. Soc.* **1996**, *118*, 9477−9483. (c) Bosch, R.; Jung, G.; Schmitt, H.; Winter, W. *Biopolymers* **1985**, *24*, 961−978. (d) Benedetti, E.; Di Blasio, B.; Pavone,V.; Pedone, C.; Santini, A.; Bavoso, A.; Toniolo, C.; Crisma, M.; Sartore, L. *J. Chem. Soc., Perkin Trans. 2* **1990**, 1829−1837.

(13) (a) Baker, E. N.; Hubbard, R. E. *Prog. Biophys. Mol. Biol.* **1984**, *44*, 97−179. (b) Schellman, C. In *Protein Folding*; Jaenicke, R., Ed.; Elsevier/North Holland Biomedical Press: Amsterdam, 1980; pp 53−61. (c) Milner-White, E. J. *J. Mol. Biol.* **1988**, *199*, 503−511. (d) Nagarajaram, H. A.; Sowdhamini, R.; Ramakrishnan, C.; Balaram, P. *FEBS Lett.* **1993**, *321*, 79−83.

(14) Karle, I. L.; Balaram, P. *Biochemistry* **1990**, *29*, 6747−6756.

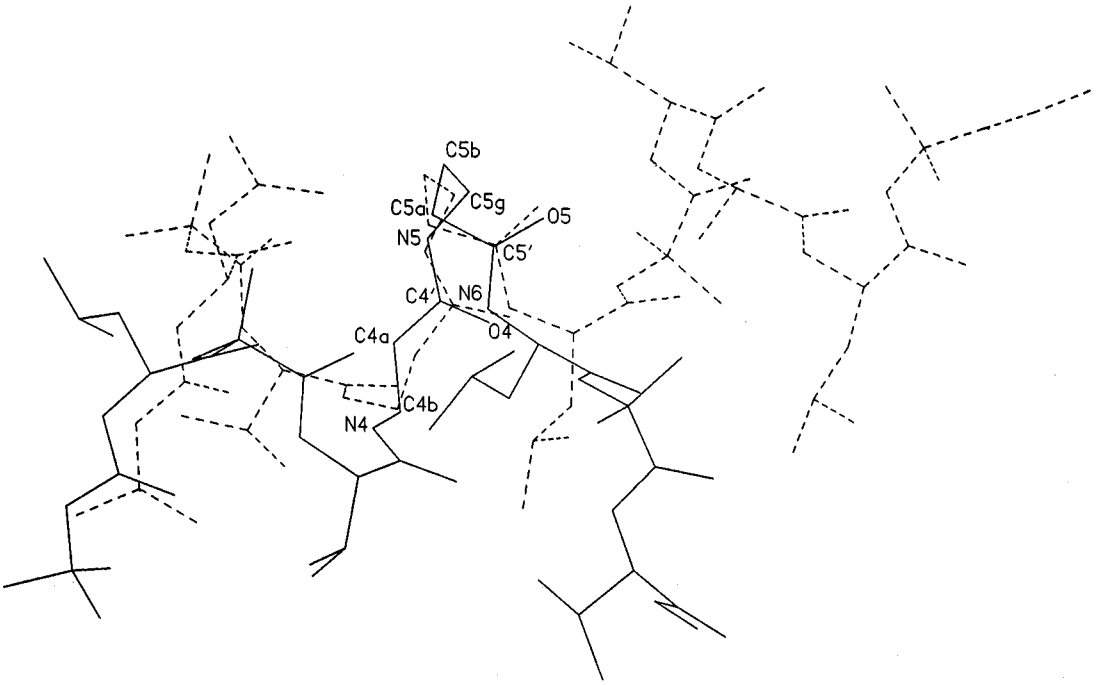

Figure 5. Differences in the conformation of **1** (solid lines) and **2** (dashed lines). A least-squares fit was made between the coordinates of the labeled atoms N4−N6.

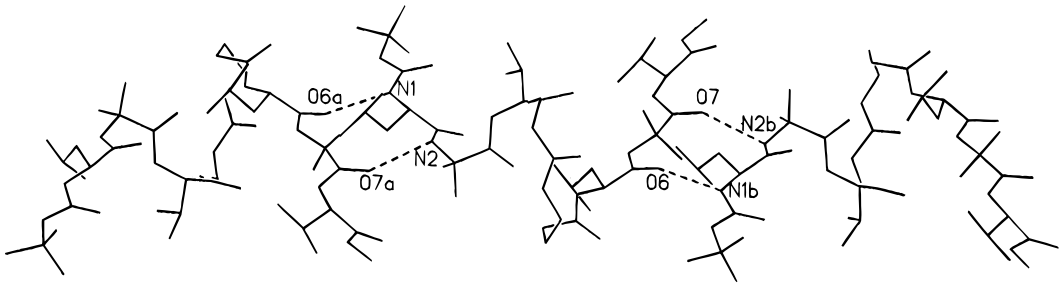

Figure 6. Stacking of helices of molecule **1** into a continuous column, held together by head-to-tail hydrogen bonds N(1)H···O(6) and N(2)H···O(7). Adjacent molecules within the column are related by a 2-fold screw.

Table 6. Comparison of Hydrogen Bonding in Helices Containing β-Ala^5-γ-Abu^5 in the Sequence

residue	type	**1**	**2**	type
Leu	head-to-tail	N(1) → O(6)	N(1) → O(9)	head-to-tail
Aib	head-to-tail	N(2) → O(7)	N(1) → O(10)	head-to-tail
Val	4 → 1	N(3) → O(0)	N(3) → O(0)	4 → 1
β-Ala	4 → 1	N(4) → O(1)	N(4) → O(0)	5 → 1
γ-Abu	external	N(5) - - - → O(9)	N(5) → O(1)	5 → 1[d]
Leu	5 → 1[a]	N(6) → O(2)	N(6) → O(3)	4 → 1[e]
Aib	4 → 1[b]	N(7) → O(4)	N(7) → O(4)	4 → 1[b]
Val	6 → 1[c]	N(8) → O(3)	N(8) → O(5)	4 → 1
Leu			N(9) → O(6)	4 → 1
Aib			N(10) → O(6)	5 → 1
Val			N(11) → O(7)	5 → 1

[a] In a 16-atom ring. [b] In a 12-atom ring. [c] With helix reversal in a 19-atom ring. [d] In a 14-atom ring. [e] In a 13-atom ring.

N(3)H···O(0) and N(8)H···O(3) are very weak because the N···O distances are >3.3 Å and the H···O distances are >2.4 Å.

The intrahelical hydrogen bonds in molecule **2** whose sequence differs from that in **1** only in the addition of the -Ala9-Leu10-Aib11- segment, alternate between the 4 → 1 and 5 → 1 type (Table 5). The two transitions between 4 → 1 and 5 → 1 hydrogen bond types occur between N(3) and N(4) where each is a donor to O(0) and between N(9) and N(10) where each is a donor to O(6). The three extra CH_2 groups inserted into the backbone cause three unusual hydrogen bonds: a 5 → 1 between N(5) and O(1) with a 14 atom ring; a 4 → 1 type between N(6) and O(3) with a 13 atom ring; and a 4 → 1 type between N(7) and O(4) with a 12 atom ring (Figure 4, parts d, e, and f, respectively). In molecule **2**, just as in **1**, the torsion angles involving the inserted CH_2 groups are approximately +60°. The only similarity between the unusual hydrogen bonds in **1** and **2** is the 4 → 1(C_{12}) type shown in the Figure 4c,f. None of these unusual types correspond to the C_{11} type for the β-Ala residue described by Lombardi et al.[1d,e] A comparison of the hydrogen bonding in **1** and **2**, represented schematically in Table 6, appears to indicate a possible facile transition between 4 → 1 and 5 → 1 hydrogen bonds. However, a measure of the large differences in conformations of the two molecules is illustrated in Figure 5, where a least-squares fit has been made between atoms N(4) and N(6). The lack of conformational correspondence accounts for the failure of a structure solution for **2** based on a vector search using a model from **1**.

Packing of the Helices. The ubiquitous head-to-tail assembly of the helical peptides[15] into a continuous column, with at least one NH···O═C hydrogen bond between an upper and lower

(15) (a) Karle, I. L. *Acta Crystallogr. B* **1992**, *48*, 341−356. (b) Karle, I. L.; Gurunath, R.; Prasad, S.; Kaul, R.; Balaji Rao, R.; Balaram, P. *Int. J. Pept. Protein Res.* **1996**, *47*, 376−382. (c) Karle, I. L.; Balaji Rao, R.; Kaul, R.; Prasad, S.; Balaram, P. *Biopolymers* **1996**, *39*, 75−83. (d) Karle, I. L.; Flippen-Anderson, J. L.; Uma, K.; Balaram, P. *J. Pept. Sci.* **1996**, *2*, 106−116.

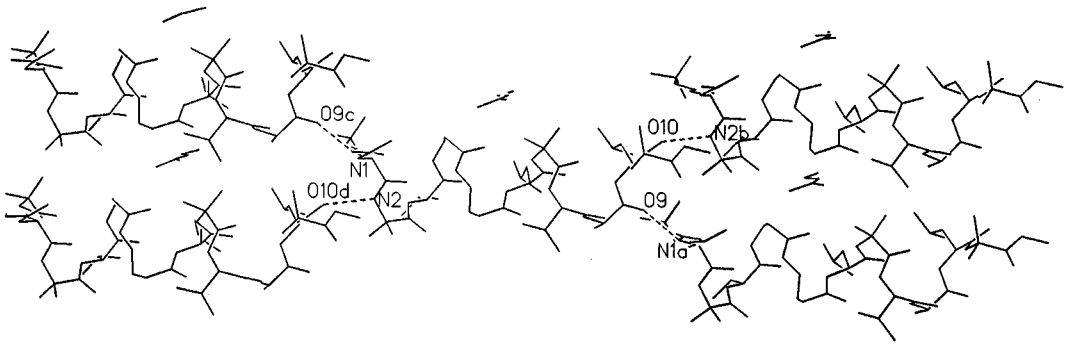

Figure 7. Head-to-tail hydrogen bonding in **2** (N(1)H···O(9) and N(2)H···O(10)) creates a checkerboard pattern. The resulting cavities between neighboring helices are filled with cocrystallized ethyl acetate molecules.

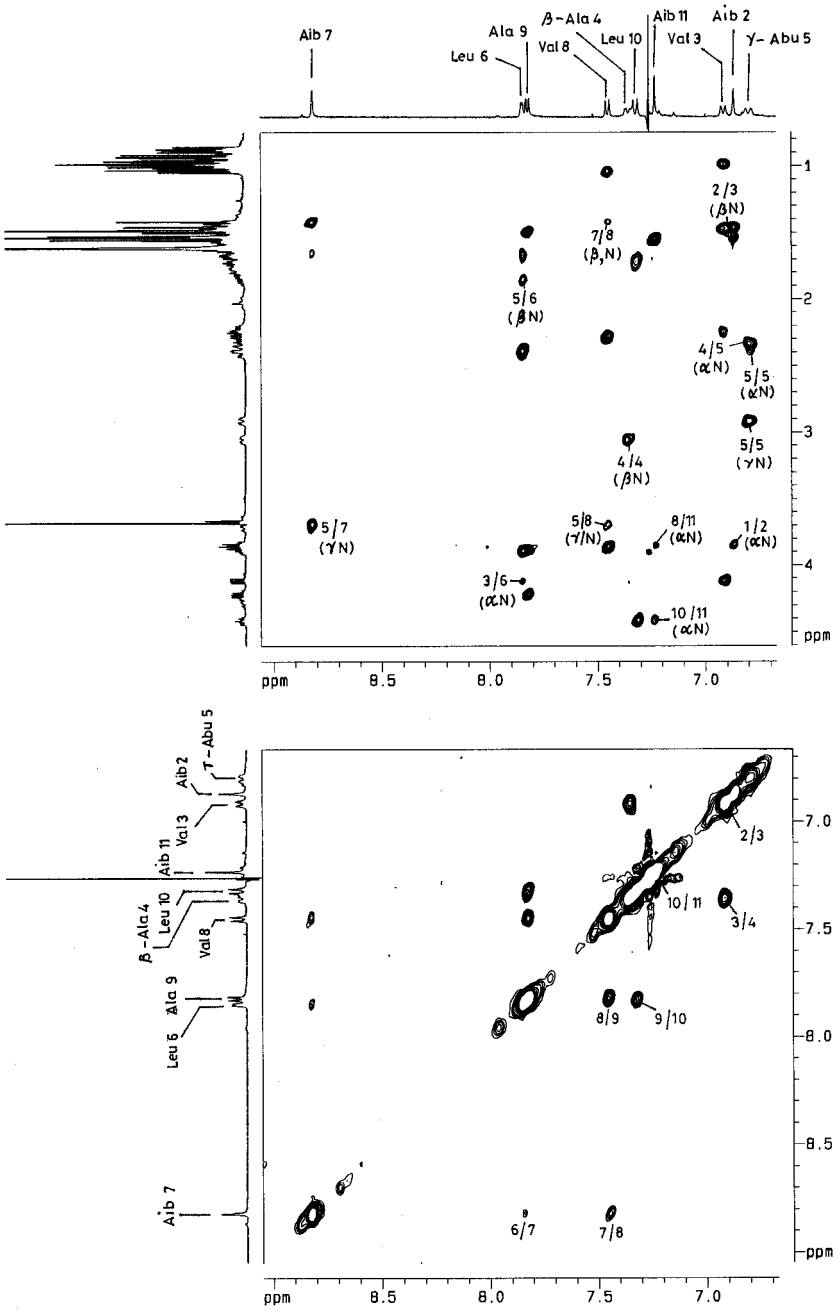

Figure 8. Partial 400 MHz NOESY spectra of the undecapeptide **2** in $CDCl_3$, showing NH−NH connectivities (bottom panel) and NH-$C^{\alpha}H/C^{\beta}H$ connectivities (top panel).

molecule in the column, also occurs in the crystals of **1**. Despite the helix reversal in **1** and consequent displacements of atoms C′(7) to C(9) from the main helix, a continuous column is formed by a 2-fold screw motion of the molecules along the *c* direction of the unit cell, held together by head-to-tail hydrogen bonding, N(1)H···O(6) and N(2)H···O(7) Figure 6.

In crystal **2**, for the head-to-tail hydrogen bonds N(1)H···O-(9) and N(2)H···O(10), the acceptors O(9) and O(10) are in

Table 7. Characteristic ^{1}H Parameters for the Undecapeptide **2** in $CDCl_2$

		δ (ppm)						NOEs[b]		
residues	NH	$C^{\alpha}H$	$C^{\beta}H$	$C^{\gamma}H$	$C^{\delta}H$	$^3J_{NHC^{\alpha}H}$ (Hz)	$\Delta\delta^a$	$d_{NN(i,i+1)}$	$d_{\alpha N(i,i+1)}$	others
Leu1	5.32	3.85	1.77	1.56	1.01	<2	1.00	w	s	
Aib2	6.88	−	1.47,1.55			−	0.59	w	−	
Val3	6.92	4.11	2.23	0.99		7.8	0.04	s	−	Val3$C^{\alpha}H$ ↔ Leu6NH (w)
βAla4	7.37	2.31, 2.40	3.05, 4.26			−	0.18	−	s	
γAbu5	6.80	2.22, 2.39	1.79, 2.02	2.90, 3.69		−	0.41	−	s	γ−Abu5NH ↔ Abu5$C^{\alpha}H$ (w)
Leu6	7.85	3.87	1.65	1.65	0.93	3	0.15	w	no NOE	γ−Abu5 $C^{\beta}H$ ↔ Leu6NH (w)
Aib7	8.81	−	1.42			−	0.11	s	−	Aib7NH ↔ γ−Abu5 $C^{\gamma}H$ (s)
Val8	7.45	3.85	2.27	1.03		6.8	0.07	s	no NOE	Val8NH ↔ γ−Abu5 $C^{\gamma}H$ (w)
Ala9	7.82	4.20	1.46			5.4	0.03	s	no NOE	
Leu10	7.13	4.42	1.70	1.78	0.88	8.0	0.04	w	w	
Aib11	7.23	−	1.55			−	0.00			Val8$C^{\alpha}H$ ↔ Aib11NH (w)

[a] $\Delta\delta$ is the chemical shift difference for NH protons in $CDCl_3$ and 10.7% $(CD_3)_2SO/CDCl_3$. Estimated error in $\Delta\delta$ is <0.02 ppm. [b] Some important interresidue NOE intensities: s = strong, w = weak.

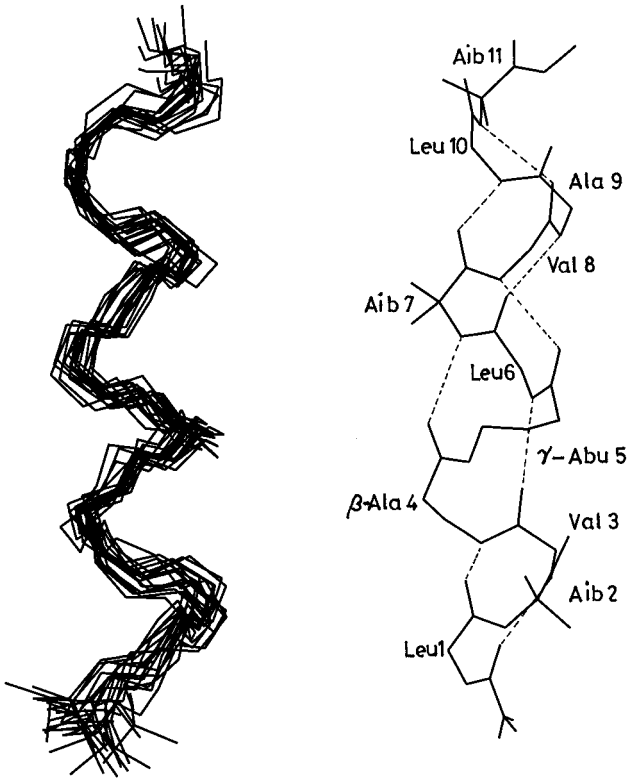

Figure 9. Superposition of 20 NMR-derived structures for undecapeptide **2** (left). The average structure of the peptide **2**, with dotted lines showing the hydrogen bonds (right).

different molecules, resulting in a checkerboard array of hydrogen-bonded molecules (Figure 7). The packing between the helices leaves open spaces into which the ethyl acetate solvent molecules are accommodated. There is no hydrogen bonding to ethyl acetate molecules. There are no unusually short C···C or C···O lateral distances between molecules.

NMR Studies of Undecapeptide 2. NMR studies in the aprotic solvent $CDCl_3$ were carried out for both the peptides **1** and **2**. In the eight-residue peptide **1**, there was severe overlap of NH chemical shifts in $CDCl_3$. Structural work in solvent was therefore confined to peptide **2**. Sequence-specific assignments were readily determined using a combination of TOCSY and ROESY experiments in $CDCl_3$. The relevant chemical shifts were summarized in Table 7. The large dispersion of NH chemical shifts is suggestive of a well-defined conformation. Solvent perturbation experiments carried out by addition of a small amount of strongly hydrogen bonding solvent $(CD_3)_2SO$ reveal that only three NH groups, viz. Leu1, Aib2, and γ-Abu5, showed appreciable solvent dependence of chemical shifts. The

Table 8. Backbone Torsion Angles[a] in the NMR-Derived Conformation of the Undecapeptide **2**

residue	Φ_{mean} (deg)	Ψ_{mean} (deg)
Leu1	−54 ± 11	−44 ± 12
Aib2	−46 ± 10	−30 ± 13
Val3	−65 ± 12	−42 ± 14
β-Ala4	−80 ± 9	−70 ± 10
γ-Abu5	−147 ± 9	−65 ± 8
Leu6	−56 ± 9	−47 ± 11
Aib7	−44 ± 8	−40 ± 14
Val8	−58 ± 7	−43 ± 8
Ala9	−60 ± 7	−25 ± 7
Leu10	−70 ± 7	−34 ± 12
Aib11	−68 ± 21	−30 ± 31

[a] The dihedral angles around the $C^{\alpha}-C^{\beta}$ bond (θ_1) of β-ala is 80 ± 9°, and the dihedral angles around the $C^{\beta}-C^{\gamma}$ (θ_1) and $C^{\alpha}-C^{\beta}$ (θ_2) of γ-Abu are 70 ± 7° and 40 ± 9°, respectively.

$\Delta\delta$ values in Table 7 establish the order of perturbation: Leu1 > Aib2 > γ-Abu5. The remaining eight NH groups appear to be inaccessible to the solvent, suggestive of their involvement in intramolecular hydrogen bond formation. A comparison with the crystal structure reveals that in solution γ-Abu5 NH may be involved in a weaker hydrogen bond interaction. The NMR analysis of inaccessible NH groups only provides an identification of potentially intramolecularly hydrogen-bonded NH groups but does not permit identification of the acceptor carbonyl residues. Further, conformational characterizations in solution therefore rely on NOE evidences. Figure 8 shows the NH−NH, NH−$C^{\alpha}H/C^{\beta}H$ region of the ROESY spectrum in $CDCl_3$. Key NOEs for determining backbone conformation are listed in Table 7. The successions of NH−NH NOEs ($N_iH-N_{i+1}H$ NOEs) for the segments 1−4 and 6−10 are supportive of a helical conformation. The NOE crosspeaks between Aib2 ↔ Val3 and Leu10 ↔ Aib11 are very close to the diagonal and are weak. These NOEs, however, are not necessary as constraints in determining the conformation of the β-Ala-γ-Abu segment. While the presence of the β-Ala-γ-Abu segment interrupts succession of short NH−NH distances in a helix, several key NOEs involving β-Ala and γ-Abu are observable in Figure 8 and listed in Table 7. These NOEs limit the range of conformational possibilities for this segment.

Assuming an idealized helical conformation around the segments 1−4 and 6−10 as indicated by the NH group solvent accessibility data and backbone NOEs, a starting model was generated (see Experimental Section) for constrained MD refinement of the structure. Figure 9 shows the superposition of twenty peptide backbone structures with an RMSD of 0.78 ± 0.05 Å. It is evident that the backbone conformation is helical. Table 8 summarizes the backbone torsion angles for the NMR-derived mean conformation, which are in good

agreement with the crystal structure. It is particularly noteworthy that the C−C torsion angles for β-Ala and γ-Abu determined by NMR (β-Ala, $\theta = 80 \pm 9°$; γ-Abu, $\theta_1 = 70 \pm 7°$, $\theta_2 = 40 \pm 10°$) are in good agreement with those determined by X-ray diffraction (β-Ala, $\theta = 78°$; γ-Abu, $\theta_1 = 62°$, $\theta_2 = 57°$).

Conclusions

The crystal structure determinations of the octapeptide Boc-Leu-Aib-Val-β-Ala-γ-Abu-Leu-Aib-Val-OMe (**1**) and the undecapeptide Boc-Leu-Aib-Val-β-Ala-γ-Abu-Leu-Aib-Val-Ala-Leu-Aib-OMe (**2**) establish that the β-Ala-γ-Abu segment can be comfortably accommodated into helical peptide structures with the additional backbone carbon atoms forming a small perturbation. The incorporation of poly(methylene) units into the helix is facilitated by the adoption of *gauche* conformations about specific C−C bonds. The observed intramolecular hydrogen bonding patterns permit most NH groups to be involved in helix-stabilizing interactions. In the case of the undecapeptide, the observed helix is robust even in solution as established by NMR studies. The ability to insert ω-amino acids into helical secondary structures, without major conformational upheaval, should have important implication for designing analogues of biologically active peptides. Protease resistance can be conferred by simple replacement of scissile peptide bonds by the corresponding, inert C−C linkage. While only simple unsubstituted achiral β- and γ-amino acids have been used in the present study, the availability of functionalized β-amino acids by Arndt−Eistert homologation of α-amino acids will undoubtedly expand the β-amino acid repertoire[16] in the future. Indeed a helical secondary structure for a hexapeptide containing all β-amino acids has been suggested on the basis of NMR studies[16] and the crystal structure of a 14-helix has been described in the solid state, as well characterized in solution, for the peptide Boc-[−NH−C_6H_{10}−C(O)−]$_6$-OBz.[17] Solution NMR studies have also been used to demonstrate the incorporation of δ-amino valeric acids into a peptide helix.[1a] Recent work has also focused on the helicity of short chain peptides formed from β-amino acids.[18] The present study is, however, the first unambiguous crystallographic characterization of β- and γ-amino acid incorporation into peptide helices. Future studies can usefully focus on the effects of selective removal of hydrogen bonds and change of register of peptide units on helix stability. The effects of incorporation of poly(methylene) units on the circular dichroism of helical peptides also merit future investigation. The availability of high-resolution crystal structure data on long modified helices as in peptide **2** can provide crucial stereochemical inputs for developing the structural chemistry of ω-amino acid containing peptides.

Acknowledgment. This research was supported in part by a grant from the Department of Science and Technology, India, by the National Institute of Health (Grant GM-30902), and by the Office of Naval Research. The use of the AMX-400 NMR spectrometer at the Sophisticated Instruments Facility, Indian Institute of Science, is gratefully acknowledged. A.P. was supported by the award of a Research Associateship from the Council of Scientific and Industrial Research, India.

Supporting Information Available: Tables of atomic coordinates, bond lengths, bond angles, anisotropic temperature factors, and hydrogen atom coordinates for peptides **1** and **2** (19 pages). See any current masthead page for ordering and Internet access instructions.

JA970566W

(16) Seebach, D.; Overhand, M.; Kühnle, F. N. M.; Martinoni, B.; Oberer, L.; Hommel, U.; Widmer, H. *Helv. Chim. Acta* **1996**, *79*, 913−941.

(17) Appella, D. H.; Christianson, L. A.; Karle, I. L.; Powell, D. R.; Gellman, S. H. *J. Am. Chem. Soc.* **1996**, *118*, 13071−13072.

(18) Seebach, D.; Ciceri, P. E.; Mark, O.; Jaun, B.; Rigo, D.; Oberer, L; Hommel, U.; Amstutz, R.; Widmer, H. *Helv. Chim. Acta* **1996**, *79*, 2043−2066.